

Understanding the Effects of Confinement and Crystallinity on HJ-Coupling in Conjugated Polymers via Alignment and Isolation in an Oriented Mesoporous Silica Host

Published as part of *The Journal of Physical Chemistry virtual special issue "125 Years of The Journal of Physical Chemistry"*.

K. J. Winchell, Matthew G. Voss, Benjamin J. Schwartz,* and Sarah H. Tolbert*

Cite This: <https://doi.org/10.1021/acs.jpcc.1c05844>

Read Online

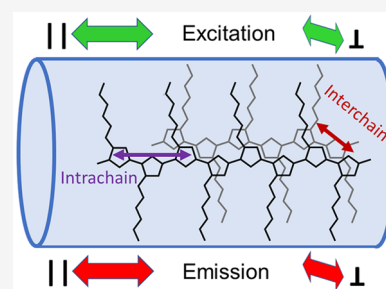
ACCESS |

Metrics & More

Article Recommendations

Supporting Information

ABSTRACT: Although there has been significant interest in the nature of exciton spatial coherence in conjugated polymers, it is usually not possible to control the extent of H- or J-coupling between polymer chains because the polymers have a naturally preferred morphology when spin-cast into films. In this work, we explore the nature of exciton spatial coherence in conjugated polymer chains that have been straightened by encapsulation in the channels of a macroscopically aligned mesoporous silica host. The small size of the pores hinders the formation of polymer crystallites, allowing us to control the polymer chain conformation without crystallinity. This provides a way for us to study the H- and J-coupling on straight polymer chains that are not crystalline, something that cannot be done with traditional film casting methods. We specifically prepare two different sets of host/guest composites using both P3HT (poly(3-hexylthiophene)) and MEH-PPV (poly[2-methoxy-5-(2-ethylhexyloxy)-1,4-phenylenevinylene]) chains as the guests. We then perform a series of polarized absorption and emission experiments on the encapsulated polymer chains, which reveal that the composite samples each contain two distinct polymer populations: a predominantly aligned population of straightened polymer chains and an isotropic population of coiled and generally isolated polymer chains. The aligned population is more ordered than the isotropic population for both polymers, an effect that is particularly pronounced for P3HT. We find that the same types of spectral changes observed when P3HT crystallizes are also present in the straightened P3HT chains and that P3HT can still exhibit H-dominant aggregation, even without extended crystallinity. In contrast, MEH-PPV exhibits enhanced J-character when the polymer backbone is aligned and straightened by the pores, with an exciton coherence size that is larger than that observed in spin-cast polymer films. This study thus provides a more fundamental understanding of the effects of backbone straightening on the aggregation behavior of both H- and J-type conjugated polymers.



INTRODUCTION

Semiconducting polymers are a widely used class of materials for many organic electronic applications, including light-emitting diodes (LEDs) and photovoltaics (OPVs), because of their low cost and solution processability.^{1–3} In addition, their solubility in many common organic solvents and thus ease of processing make it possible to easily manipulate their morphology to improve device performance via simple methods such as the choice of casting solvent, thermal annealing, or solvent annealing.^{4–7} In these types of polymers, small morphology changes can have large effects on the nature of exciton formation, which in turn directly affects the performance of OPVs and LEDs. Semiconducting polymer excitons are particularly sensitive to the local morphology because they are capable of delocalizing in multiple directions, both along the polymer chain and across the π -stacks between polymer chains.^{8,9} In highly ordered polymers, excitons can maintain spatial coherence well in both directions.⁸ This

increased exciton spatial coherence is crucial for increased charge separation and thus device performance in OPV applications;^{10,11} changes in the exciton emission yield also directly affect LED performance.

Because exciton formation is a crucial step in organic electronic device performance, there is much interest in studying the fundamentals of semiconducting polymer excitons and the ways in which manipulating polymer morphology affects excitons. Exciton coupling in small molecules has long been understood via the model of H- and J-aggregates

Received: June 30, 2021

Revised: September 24, 2021

presented by Kasha and Hochstrasser.^{12,13} In this model, a material that is described as an H-aggregate lies with its chromophores side-by-side and a J-aggregate material has chromophores that lie head-to-tail. Much of the groundwork for understanding conjugated polymer excitons has been laid out by Spano and co-workers, who have demonstrated that excitations in semiconducting polymers can be understood via a modified H- and J-aggregate model using the concept of HJ-aggregate hybrids.^{8,14–17} In polymers, J-aggregation is analogous to coupling along the chain while H-aggregation arises from interactions in the π -stacking direction that allows for interchain coupling. In reality, both types of coupling are present in most conjugated polymers, and there are direct interactions between the two.

One of Spano and co-workers' key contributions is the demonstration that the coupling between excitons and the vibrations of the semiconducting polymer backbone creates clear absorption and emission spectral signatures that demonstrate whether H- or J-like aggregation behavior is dominant in a given polymer.^{18,19} In polymers where J-aggregate behavior dominates, the 0–0 peaks in both absorbance and fluorescence are prominent, whereas in H-aggregate-like polymers, the 0–0 peak is nominally disallowed, so that the 0–1 peak is the main feature of the absorption and emission spectra. Seeing these readily observed changes in the spectra makes it straightforward to assess how changes in morphology affect the nature of excitons in semiconducting polymers.

One of the most common polymers that has been studied by using this HJ-aggregate model is poly(3-hexylthiophene) (P3HT). P3HT is ubiquitous in the field of semiconducting polymers and has been used in a wide variety of devices including OPVs and thermoelectrics;^{20–22} P3HT is particularly appealing for study because of its relatively high degree of crystallinity in films. Because of its strong interchain interactions in the π -stacking region of the crystallites, P3HT is a predominantly H-aggregate-like polymer, which is reflected in its spectroscopy as the 0–1 vibrational peak dominates in both the absorption and emission spectra.

In contrast, the HJ-aggregate model also can be used to study materials like poly[2-methoxy-5-(2-ethylhexyloxy)-1,4-phenylenevinylene] (MEH-PPV),^{23,24} which because of its branched side chains is poorly crystalline and thus shows more J-aggregate-like behavior with enhanced 0–0 absorption and emission peaks. For example, it has been shown experimentally by Schwartz and co-workers that MEH-PPV films made by using different processing conditions (e.g., casting the films from different solvents) have different spectral line shapes with different vibronic peak progressions; the changes in spectroscopy could be used to explain changes in how these same films performed as the active layers in polymer-based LEDs.^{25,26} This means that MEH-PPV provides a nice contrast to P3HT for studying how intra- and interchain coupling affects the properties of the excited states of conjugated polymers.

One common way that spectral signatures and the HJ aggregate model have been applied, particularly to P3HT, is by using the 0–0/0–1 absorbance peak intensity ratio as a proxy for the degree of crystallinity in P3HT films.^{27–29} Spano has shown that increased crystallinity of P3HT results in an increase in the 0–0 vibronic peak intensity.^{30,31} This may initially seem counterintuitive because P3HT has strong π -stacking behavior and is traditionally known as an H-aggregate polymer, but an increase in the 0–0 transition corresponds to

an increase in intrachain coupling and signifies more J-aggregate-like behavior. The explanation for this behavior is that even the amorphous parts of P3HT (and also MEH-PPV)^{26,31} films have some interchain coupling, so the chain straightening caused by increasing the crystallinity of the film causes a greater increase in intrachain coupling than interchain coupling. As evidenced by the presence of a π -stacking X-ray diffraction peak even in materials like disordered regiorandom P3HT,³² all conjugated polymers, even disordered ones, are capable of some interchain coupling, but crystallinity is generally required to increase intrachain coupling to produce the corresponding J-aggregate-like absorbance features.

All of this brings up the question of the general relationship among crystallinity, order, and aggregation behavior in conjugated polymers. Are polymers like P3HT always H-aggregate-like and polymers like MEH-PPV usually J-aggregate-like? Does crystallinity drive an increase in H-aggregation in addition to J-aggregation? Do P3HT and related polymers' propensity to π -stack drive their crystalline behavior? These questions are difficult to answer because, until now, there has not been a way to separate aggregation and crystallinity in semiconducting polymers so that they can be studied independently. There have been studies of P3HT nanofibers that have shown that in some circumstances P3HT can exhibit more J-aggregate behavior, but the exact microstructure of the P3HT chains in the nanofibers is unknown and, in some cases, nanofiber formation is driven by crystallization.^{33–36}

In this paper, we present a novel method for separating aggregation and crystallinity in ordered systems of conjugated polymers. To do this, we have designed a host–guest system based on an anisotropically aligned mesoporous silica host,^{37–43} into which polymer guest chains can be infiltrated.³⁷ This system forces polymer chains to be aligned and straight—but generally not crystalline—due to spatial confinement that allows only 3–5 polymer chains to fit in each pore.³⁷ Because the optical transitions of semiconducting polymers are aligned along the backbone of the polymer, we can selectively study the spectroscopy of the most aligned and ordered chains by polarizing the light parallel to the direction of the pores. Past studies have demonstrated that it is possible to infiltrate polymers into aligned mesoporous hosts and that the chain conformation (straight or coiled) and aggregation (isolated or aggregated) can be controlled by the pore size⁴⁴ and can be used to spatially control exciton migration.⁴⁵ By use of optimized pore sizes, it can be shown that the incorporated polymer chains can have a high level of structural anisotropy,³⁷ that exciton migration along the polymer backbone takes place at a different rate than between polymer chains,⁴⁶ and that polymers within such porous films form graded-index waveguides that can produce highly polarized amplified stimulated emission (ASE).⁴⁷

The key benefit of this group of samples is that they allow for the ability to study polymer chains that are forced to be straight and close enough to other polymer chains to experience coupling but which do not have their coupling behavior dominated by crystallinity and the π -stacking interactions that typically accompany polymer ordering. Isolated straight chains can exhibit exciton migration along the chain, but understanding the roles of intra- vs interchain coupling is not possible without the presence of other polymer chains. Most previous studies altered the coupling by allowing the polymer chains to crystallize.^{8,9,11,12} However, this means

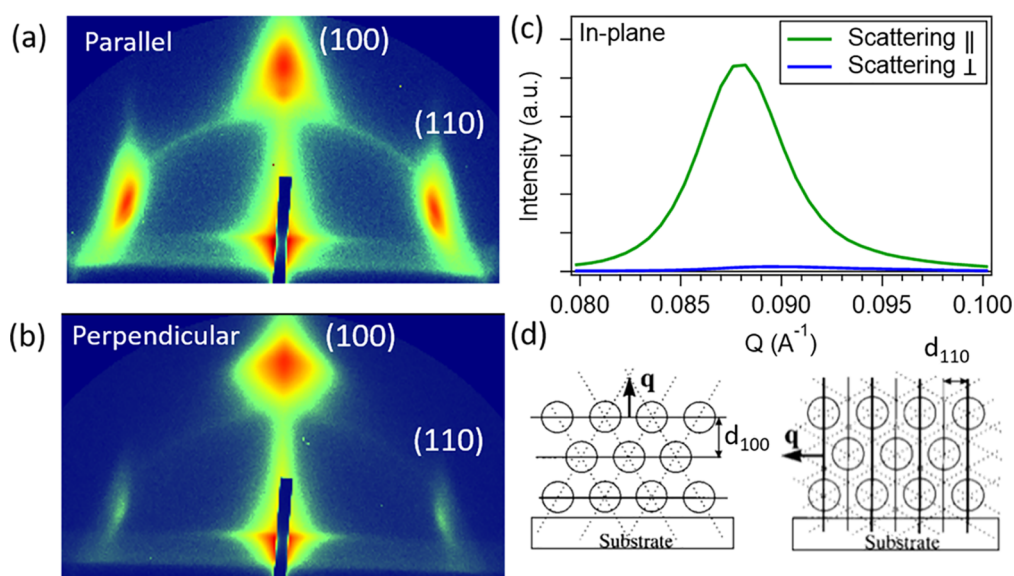


Figure 1. GISAXS of the aligned mesoporous silica host with the axis of the pores (a) parallel to the incoming X-ray beam and (b) perpendicular to the direction of the beam. The integrated in-plane peak intensity (c) shows a high degree of anisotropy, with an 18:1 alignment ratio. (d) A structure cartoon demonstrating the reason for in-plane anisotropy in the scattering of the (110) peak. Cartoon adapted from ref 38.

that the H- and J-aggregate behavior in such samples is dictated by the particular crystalline polymorph that is formed, which would leave us unable to specifically study the effects of simple chain straightening on exciton coupling and migration. Instead, encapsulating of the polymers in the channels of the aligned mesoporous silica hosts allows direct access to study the effects of H- and J-aggregation on ordered polymer chains without the presence of crystallinity. This means we can separate the coupling effects caused by crystallinity from those induced by just straightening the chain. These samples therefore create a type of HJ-coupling than cannot be observed in other types of polymer films. In addition, because the polymer chains are straight and are macroscopically aligned with the axis of the pores, we can use polarized light to selectively study these highly ordered chains.

In this study, we compare the behavior of two different conjugated polymers, P3HT and MEH-PPV, that have been straightened and ordered by incorporation into our aligned mesoporous silica hosts. After performing a careful polarized spectroscopic analysis, we find that these host/guest materials contain two distinct populations of polymer chains: one population with straightened chains that are highly aligned along the pore direction and a second population of chains with an isotropic distribution that tend to be coiled and isolated from each other. Previous studies on polymer films have not been able to examine these two populations individually, yet our novel system allows us to study the ordered and isotropic regions individually. By comparing the behaviors of these populations in our aligned mesopore system for these two well-studied, yet very different polymers in terms of their aggregation and crystallinity behavior, we can isolate how the environment of a conjugated polymer affects its HJ-coupling. We find that chain straightening is more important for controlling along-the-chain coupling than crystallinity; in other words, crystallinity can aid in straightening polymer chains, but straightening the chains without crystallinity leads to the same types of changes in the polymer's spectroscopy. We also see that interchain interactions can happen without polymer crystallinity and that alignment in pores can either

increase or decrease the degree of energetic spatial disorder depending on the natural environment of the polymer in a spin-cast film. All of the findings can help us understand how to design materials for future applications with desired degrees of along-the-chain and between-chain interactions.

METHODS

We synthesized our aligned mesoporous silica films via a surfactant-templating method that has been reported previously.^{38,39} In this method, the driving force for anisotropic alignment is the interaction of the surfactant template with a rub-aligned polyimide film. The result is an ordered porous material with hexagonally arranged long, straight pores.³⁸ All of the pores lie in the plane of the film, and while the film is polycrystalline, the pore axis of each domain lies in roughly the same direction because of the aligning polyimide film.³⁸ To verify the anisotropy of our host films, we performed grazing-incidence small-angle X-ray scattering (GISAXS). As demonstrated in Figure 1, we can measure the scattering pattern with the X-ray beam both parallel (Figure 1a) and perpendicular (Figure 1b) to the axis of the pores. As expected, this rotation does not affect the out-of-plane scattering (Figure 1a). However, when looking at the in-plane scattering (Figure 1b), the intensity is greatly reduced when the X-rays are incident on the sample perpendicular to the pore direction, as expected for an aligned system. Integrating the relative peak intensities, as shown in Figure 1c, yields an anisotropy ratio for these films of 18:1, indicating that the pores are indeed highly aligned. From the peak position at 0.088 \AA^{-1} , we can also determine that the center-to-center distance between the pores is $\sim 7 \text{ nm}$ (Figure 1d). Importantly, it has been shown previously that there are random holes in the walls of the hexagonally arranged pores that allow guest molecules to be diffused into the pores from the top, despite the fact that the pore axis lies in the plane of the film.³⁹

Once synthesized, semiconducting polymers can be incorporated into the porous film by first adding a hydrophobic coating to the inner surface of the pores and then soaking the porous film in a conjugated polymer solution.³⁷

The polymer solution is then slowly concentrated by evaporation to drive the polymer chains into the pores. This results in incorporated polymer chains that are straight and macroscopically aligned within the pores.

RESULTS AND DISCUSSION

For polymer chains incorporated and aligned within the pores, we can determine the degree of anisotropy simply by comparing the intensity of the optical absorbance or emission polarized parallel and perpendicular to the axis of the pores. Figures 2a and 2b show that both P3HT and MEH-PPV have

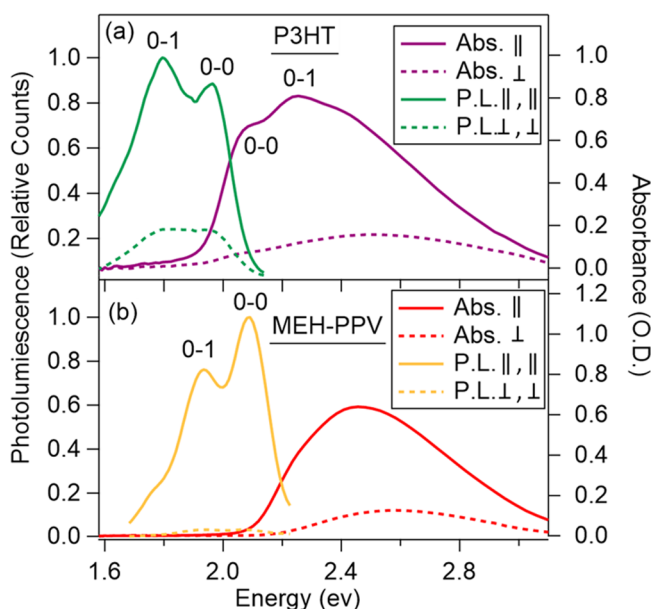


Figure 2. Absorbance and photoluminescence of P3HT (a) and MEH-PPV (b) aligned within mesoporous silica demonstrating the host-induced polymer anisotropy. The solid curves show the spectra when the light is polarized parallel to the pore direction, and the dashed curves show the spectra when the light is polarized perpendicular to the pore direction. The emission spectra are collected by using the same polarization as the excitation light (cross-polarized excitation/emission combinations are shown in Figure S2).

large intensity differences between their parallel and perpendicular emission, indicating that both polymers have been aligned in the porous host films. Because the absorption and emission dipoles of both P3HT and MEH-PPV are roughly aligned with the backbone of the polymer,^{45,48} we can conclude that the polymer chains absorbing and emitting light parallel to the pores are aligned within the silica host. The remaining polymer population, which absorbs and emits light perpendicular to the pores, must be coiled and thus more isotropically distributed within defects in the porous silica films. This means that we can selectively study the emission of the ordered straight and coiled amorphous polymer chromophore populations by simply choosing the appropriate excitation polarization.

Figure 3 shows the perpendicular and parallel absorbance data normalized to better determine the effect of aligning and confining the polymer chains on their aggregation behavior. In general, the population of polymer chains that absorb light parallel to the pore axis are the most ordered and thus will not have their conjugation disrupted by bends in the chain. For

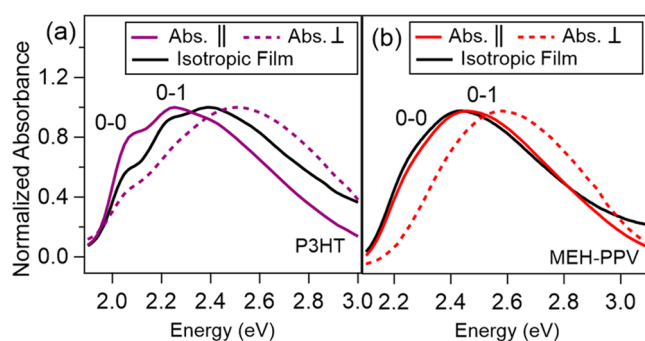


Figure 3. Normalized polarized absorbance of (a) P3HT and (b) MEH-PPV chains encapsulated in the aligned mesoporous silica host. The solid colored curves show the absorption spectrum for light polarized parallel to the pore direction, while the dashed curves show the absorption spectrum for light polarized perpendicular to the pore direction. This is the same data shown in Figure 2 but normalized for ease of comparison. For comparison, the normalized absorption spectrum for an isotropic spin-cast film is shown in black for each polymer. For both host/guest films, the polymer chains that absorb the perpendicularly polarized light do so at higher energy due to the relative lack of exciton spatial coherence compared to the ordered and aligned chains that absorb light polarized parallel to the pore direction. The ratio of the 0–0 to 0–1 vibronic absorption features also changes with the light polarization, particularly for P3HT. Compared to the isotropic spin-cast film, the P3HT encapsulated film has higher-intensity 0–0 and 0–1 vibronic features for the absorbance spectrum collected with the light polarized parallel to the pore direction.

P3HT (Figure 3a), we can see that the more ordered chains have an increased 0–0 absorption peak; this is very similar to the way that increased crystallinity results in enhanced 0–0 peak absorption intensity in bulk P3HT films.^{49,50} Figure 3a also shows that the P3HT 0–0 absorption peak is more enhanced for the ordered chains in the aligned mesopores than it is in isotropic bulk P3HT films. In our aligned host/guest samples, it is important to note that the observation of the enhanced 0–0 absorption cannot be due to increased polymer crystallinity because there are at most 3–5 chains per pore, so that there are simply not enough polymer chains to be truly crystalline, and the spatial confinement of the pore likely prevents the polymer chains from packing the way they would in a bulk film. Thus, the enhanced 0–0 absorption must arise from the straightening of the P3HT chains, as discussed further below. We also observe that for P3HT in the aligned pores the absorption parallel to the pore direction is shifted to lower energy than that in the perpendicular direction, indicating that, as expected, chains absorbing parallel to the pore axis have increased exciton spatial coherence.

Figure 3b shows that in a similar fashion MEH-PPV polymer chains that absorb light parallel to the axis of the pores also have their absorption shifted to lower energy compared to the chains that absorb perpendicular to the pore axis, again consistent with the idea of enhanced exciton spatial coherence for chains that are straightened by the pores. We also see that there is slightly enhanced vibronic structure in the absorption spectrum polarized parallel to the host pores relative to that polarized perpendicular to the pores. However, compared to P3HT, MEH-PPV has such poorly defined vibronic structure in its absorption spectrum that there is little direct information we can extract simply by visually examining the absorption.

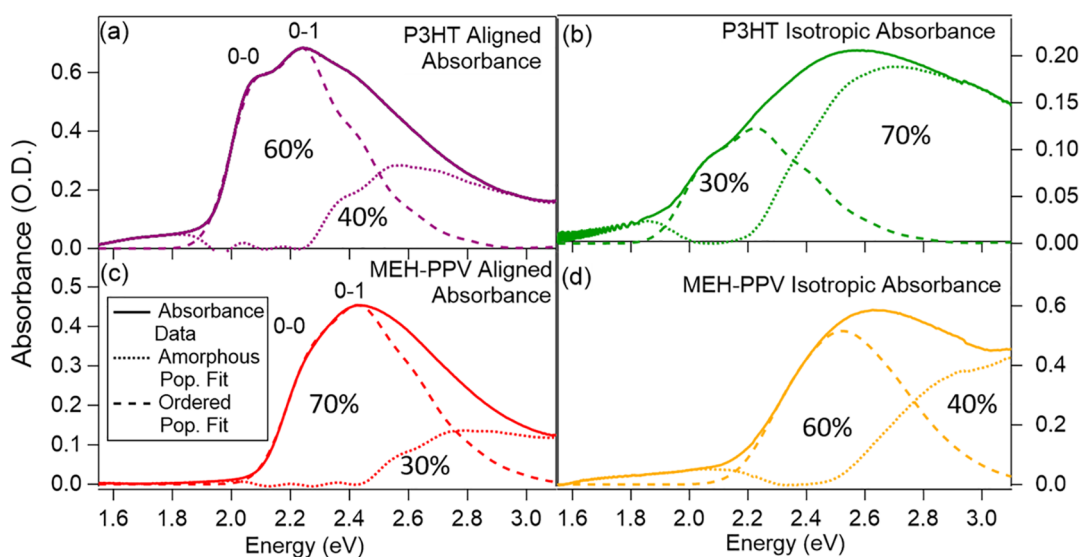


Figure 4. Separation of the absorption of conjugated polymer guests (a, b: P3HT; c, d: MEH-PPV) in the aligned mesoporous silica hosts into aligned and isotropic populations. The entire perpendicularly polarized absorption is presumed to come from the isotropic population (solid curves in panels b and d). The absorption spectrum of the aligned population is then determined by subtracting the isotropic absorption from the parallel-polarized absorption to produce the solid curves in panels a and c. These absorption spectra are then fit to the HJ-aggregate model³¹ to determine the fraction of the absorption in each case that results from ordered aggregated chains (dashed curves in each panel) and disordered amorphous chains (dotted curves in each panel).

To learn more about the degree of order of the P3HT and MEH-PPV chains in the aligned mesoporous silica hosts, we modeled the polarized absorption spectra as shown in Figure 4. Specifically, each encapsulated polymer sample was modeled as having two populations: one composed of straightened polymer chromophores that are aligned by the pores and one consisting of isotropic polymer chromophores that reside in the interstitial spaces in the hosts or which manage to coil within the pores. The entirety of the absorption perpendicular to the pore axis is attributed to this isotropic population, which is expected to absorb equally strongly in the perpendicular and parallel directions. The absorption of the population of polymer chains aligned along the pore axis is then obtained by subtracting the isotropic absorption component from the measured parallel-polarized absorption spectrum.

We then further decomposed the spectra of the aligned and isotropic polymer populations in each sample into ordered and disordered components using the HJ-aggregate model developed by Spano et al.^{27,51} This model assumes that there is an ordered, aggregated component to the absorption spectrum of each population that has a well-defined vibronic progression with relative peak intensities determined by how spatially coherent the exciton can be in the aggregate. The remaining absorption then results from the disordered, amorphous part of that population. The details of the Poissonian vibronic progression predicted for the ordered chains by the model are given in the Supporting Information. When we fit the model to each of the two different populations (aligned and isotropic), we find that the aligned population in the P3HT host/guest sample consists of approximately 60% ordered chains and 40% disordered chains (Figure 4a). In contrast, the isotropic P3HT population is only 30% ordered and 70% disordered, as seen in Figure 4b.

Figure 4 also shows that the difference in ordering between the aligned and the isotropic populations of the host-encapsulated MEH-PPV is less pronounced than that seen with P3HT. The fits to the HJ-aggregate model show that the

aligned MEH-PPV population is roughly 70% ordered (Figure 4c), while the isotropic MEH-PPV population still shows 60% ordered character (Figure 4d). We note that the vibronic structure in the MEH-PPV absorption spectrum is intrinsically less pronounced than that in the P3HT absorption. This is why we find high ordered fractions, even though the MEH-PPV absorption spectra do not show sharply defined vibronic peaks.

To better understand the degree of ordering in the MEH-PPV host/guest samples, we compare the fits to the absorption spectrum of MEH-PPV encapsulated in the aligned silica pores to that of the spin-cast MEH-PPV bulk film shown in Figure 3b. We find that the fraction of ordered chains in the bulk spin-cast film is similar to that of the aligned population in the pores, although the vibronic peaks are broader and blue-shifted in the spin-cast film (Figure S1b, 70% ordered for the spin-cast film and 70% for the aligned polymers in the porous host). In contrast, Figure S1a shows that for P3HT encapsulation in the aligned porous silica host results in an enhanced ordered fraction relative that in a bulk spin-cast P3HT film (50% ordered for the spin-cast film versus 60% for the aligned polymers in the porous host).

These observations indicate that straightening J-aggregate-dominant MEH-PPV chains by encapsulation does not affect the fraction of polymer chain segments that are ordered, while straightening H-aggregate-dominant P3HT has a large effect on the degree of ordering. This conclusion is reinforced by the fact that the absorption of neat P3HT films seen in Figure S1a is red-shifted relative to the aligned P3HT population in the pores, while the opposite is observed for MEH-PPV in Figure S1b. Apparently, aligning and confining the backbone of MEH-PPV aid in exciton spatial coherence, while aligning and confining the backbone of P3HT limit exciton spatial coherence. This is because in J-aggregate-dominant MEH-PPV the chains in bulk films have reduced exciton spatial coherence, presumably because the branched side chains interfere with exciton coherence between neighboring chains. Straightening these chains in pores thus enhances the along-

the-chain coupling, increasing the overall degree of order. In contrast, H-aggregate-dominant P3HT chains have ordered excitons that are spatially coherent both along and between the chains in bulk films. The increased ordering that takes place by straightening the chains in the aligned silica hosts is overcompensated by the loss of some 2-D spatial coherence because the chains in the pores are isolated.

With this understanding from the polarized absorption spectra of how aligning polymer chains without crystallinity affects the degree of order, we turn next to Figure 5, which

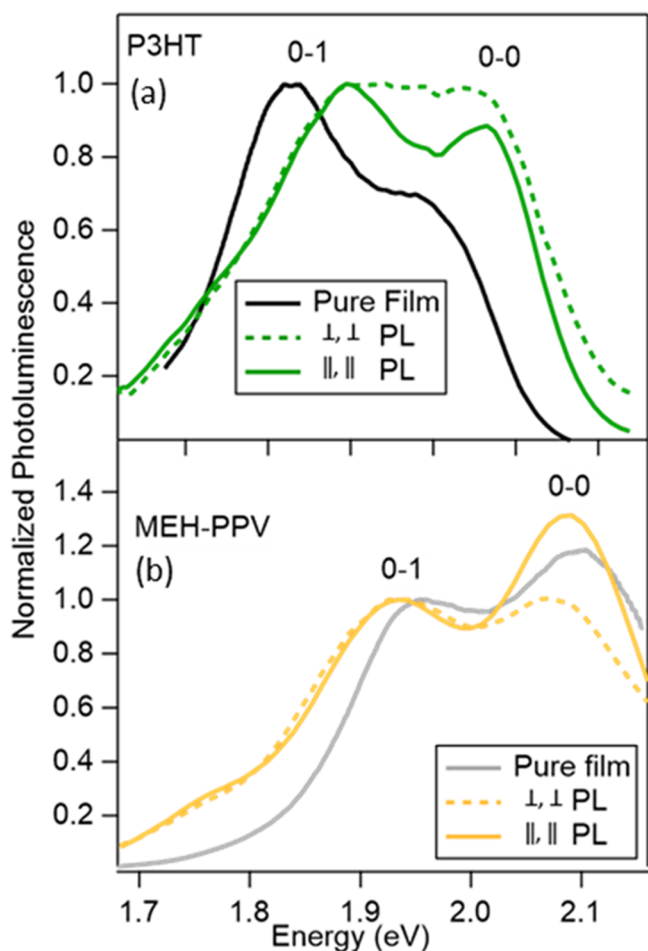


Figure 5. Normalized polarized photoluminescence from (a) P3HT and (b) MEH-PPV in different environments: bulk spin-cast films (black curves), chains aligned along the direction of the pores in the silica host (solid colored curves), and chains with isotropic emission in the silica host (dashed colored curves). The change in PL 0–0/0–1 ratios shows that the degree of HJ aggregation for each polymer varies with the different environments.

compares the polarized photoluminescence (PL) from the host/guest samples to those from spin-cast bulk films. As with Figure 2, Figure 5 explores the emission of polymer chains that both absorb and emit light parallel to the pore axis to those that both absorb and emit perpendicular to the pore axis (cross-polarizations are also possible and will be discussed later). Figure 5a shows that the relative heights of the 0–0 and 0–1 PL peaks of P3HT bulk spin-coated films and the aligned polymer chains in the silica pores are quite similar, indicating that there is little change in the aggregation behavior of P3HT in these two environments. Moreover, the fact that the 0–1

emission peak has the highest intensity in the aligned pores indicates that P3HT can have H-aggregate-dominant behavior even when extended crystallinity is not possible: the non-crystalline pore environment still allows for some degree of 2-D exciton spatial coherence. In contrast, the least ordered chains, which absorb and emit light perpendicular to the pore axis, show a decrease in the PL 0–1/0–0 peak ratio, showing that the polymer in this environment is hindered in its ability to have excitons remain spatially coherent between chains.

Similar to what we saw for the absorption spectra, Figure 5a shows that the most ordered P3HT chains within the pores have an emission spectrum that is shifted to higher energy relative to pure P3HT films. Although part of this shift may come from a change in the dielectric environment of the chains when they are surrounded by silica, we attribute the bulk of this shift to increased quantum confinement of the exciton. P3HT excitons in crystalline films tend to maintain spatial coherence in two directions, but the small diameter of the pores allows for so few chains to interact that less interchain exciton spatial coherence is possible in the pores than in a bulk film.

Interestingly, the MEH-PPV PL data in Figure 5b shows the opposite trends to those observed for P3HT in almost every way. Most notably, the most aligned polymer chains, those that absorb and emit parallel to the pore axis, have an increased PL 0–0 peak intensity relative to bulk films. This increase suggests that even though MEH-PPV is traditionally a J-aggregate-dominant polymer, the exciton coherence length in bulk films is relatively short and thus can be increased by forcing the polymer chains to be straight over a longer length scale. In addition, we can see even within this confined environment, where the chains are forced to be physically close to each other due to alignment, MEH-PPV chains within the pores cannot be induced to show strong interchain interaction or π -stacking (i.e., more H-aggregate-like behavior). This idea is consistent with previous studies that used temperature to induce order and chain straightening for MEH-PPV: even when cooled to 10 K, bulk MEH-PPV films continued to show properties similar to those of single chains, with relatively little interchain interaction.^{14,23} Finally, the most ordered MEH-PPV chains within the pores have an emission spectrum that is shifted to lower energy relative to pure MEH-PPV films. Although this may be partly a dielectric effect, it indicates that the straightening of the chains along the pores results in reduced quantum confinement for MEH-PPV in pores, despite the very small pores size, in direct contrast to the behavior observed for P3HT.

To better understand how confinement affects the along-the-chain versus the between-the-chain interactions, we analyzed the PL spectra to quantify the degree of H-aggregation for P3HT (Figure 6a,b) and MEH-PPV (Figure 6c,d) in the different environments. Similar to how we analyzed the absorption data above, we identified two distinct populations of polymer chains contributing to the polymer PL spectra in the silica host. Specifically, we assumed one largely HJ-aggregated polymer population that is aligned with the pore axis (dashed lines, Figure 6) and an isotropic population (dotted lines, Figure 6). Based on the theory of HJ-aggregates from Spano and co-workers, the PL spectra of each of these components can be modeled as a series of evenly spaced Gaussians weighted by a factor of frequency cubed, as detailed in the Supporting Information.⁵² The model for the emission is different from the absorption because only the 0–0 emission

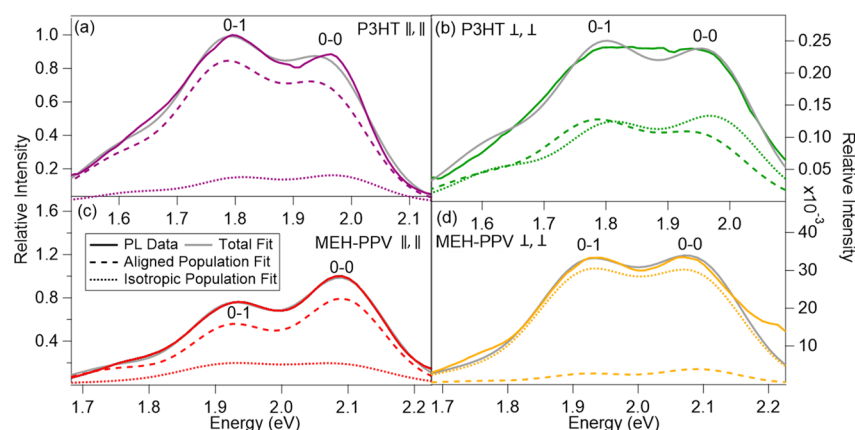


Figure 6. Normalized photoluminescence (solid curves) for P3HT (a, b) and MEH-PPV (c, d) in the aligned silica host that both absorb and emit parallel (a, c) and perpendicular (b, d) to the pore axis. These data are also shown in Figure 2 in un-normalized form. The thin gray curves show fits to the PL spectra assuming two polymer populations that emit according to the model of Spano and co-workers;⁵² the dashed curves show the aligned component while the dotted curves show the isotropically emitting component. For both polymers, the differences in spectral shape of the two components directly reflect changes in the along-the-chain (J-like) vs between-the-chain (H-like) coupling.

band is strongly affected by the degree of aggregation. In the emission model, the PL 0–1 to 0–0 intensity ratio is used to extract the exciton coherence number, which is a measure of the number of chromophores over which an exciton can remain wavelike, while the PL 0–1 to 0–2 intensity ratio is more sensitive to intrachain or J-like coupling. In this way, the HJ nature of the exciton for polymer chains that are straightened but not crystallized can also be examined by using the PL data.

We begin by considering the isotropic emission component of both polymers. For MEH-PPV, the low PL 0–0/0–1 peak ratio of the isotropic population (dotted curves in Figures 6c,d) indicates more H-like behavior than is typically seen in poorly crystalline polymers like MEH-PPV. We do not believe that this reflects an increase in π -stacking or interchain coupling, but instead we attribute this to disruption of the conjugation along the backbone and therefore a loss of the end-on chromophore J-aggregate coupling. In contrast, the PL 0–0/0–1 peak intensity ratio for the isotropic population of P3HT in the silica host (dotted curves in Figures 6a,b) is larger than that of the aligned polymer population in the pores (dashed curves in Figures 6a,b). This suggests that in a dominantly H-like polymer like P3HT the larger disorder of the isotropic P3HT population in the pores does affect the π -stacking and therefore reduces the H-like chromophore coupling.

Next, we examine the population of polymer chains that are aligned with the axis of the pores. For the aligned population of P3HT chromophores, the dashed curves in Figures 6a and 6b show that the PL 0–1 peak is dominant, indicating that some π -stacking behavior is maintained, although significantly less than in bulk films (cf. Figure 5a). In contrast, MEH-PPV polymer chains that are aligned, as seen in the dashed curves in Figures 6c and 6d, show J-aggregate-like behavior with a dominant PL 0–0 peak, which reinforces our conclusion that causing MEH-PPV chains to be highly aligned and straightened does not result in an increase in π -stacking or H-like coupling.

We can expand our analysis of the PL to compare the exciton coherence numbers^{53,54} of the different polymer populations in the aligned mesoporous silica hosts. For the aligned population of MEH-PPV, the ratio of the PL 0–1 to

0–0 peak intensities yields a coherence size of 1.35 chromophore units, while the isotropic population has a coherence number of ~ 1 , implying that the isotropic fraction has truly isolated chromophores. We find that spin-coated MEH-PPV films (Figure S3c,d) have an exciton coherence number of 1.15 chromophore units, indicating that although H-aggregation is not apparently induced by spatial confinement, straightening of the polymer chains still causes the exciton coherence number to increase. Unfortunately, in H-dominant aggregates such as P3HT, although the PL 0–0 to PL 0–1 ratio is sensitive to the exciton coherence number, the ratio also depends strongly on destructive interference between polymer chains in the π -stacks; this prevents extraction of coherence number values from the PL 0–0 to PL 0–1 ratio for P3HT.

We can also compare the PL data in Figure 6, where the excitation and emission light are polarized in the same direction, to the case where the excitation and emission polarizations are crossed, shown in Figure S2. Unlike the emission probed with the same polarization as the excitation light, which probes the different polymer populations, the PL measured with crossed polarizers should predominantly report on excitons that have undergone energy transfer between populations. For P3HT, the PL spectrum with the excitation and emission polarizations parallel to the pore direction consists 95% of emission from the aligned population (Figure 6a), with only a small amount from the isotropic population, but all three of the other polarization combinations show roughly equal amounts of emission from the two populations (Figure 6b and Figure S2a,b). This suggests that these three polarization combinations are dominated by emission from the isotropic population and that the isotropic population can undergo energy transfer to the aligned population.⁴⁵ This makes sense given that the isotropic population has coiled polymer chains with higher-energy excitons than the straight chains in the aligned population.⁴⁵

For MEH-PPV, the behavior of the emission under cross-polarizations is somewhat different. With the excitation polarization perpendicular to the pore direction, the emission spectra (Figure S2d) show roughly equal amounts of the aligned and isotropic populations, similar to P3HT. For samples with the excitation polarization parallel to the pores

(Figure 6c and Figure S2c), however, emission from the aligned population is strongly dominant in the parallel excited and parallel polarized emission spectrum (Figure 6c), but the perpendicularly polarized emission spectrum is almost entirely dominated by the isotropic population (Figure S2c). This is because for the MEH-PPV chains in the aligned porous silica host energy transfer facilitated by π -stacking is less facile, so the only way to get perpendicularly polarized emission following parallel-polarized excitation is to have truly isolated (and thus isotropic) chains with transition dipoles that are oriented neither parallel nor perpendicular to the pores.

Finally, we can combine the information from the model fits of the PL and absorption spectra to obtain an estimate of the spatial correlation of the energetic site disorder of the aligned and isotropic polymer populations. In the HJ-aggregate model, the energetic spatial correlation parameter, β ,⁵⁵ is defined by eq S6, and the way we calculated it is described in more detail in the Supporting Information. The value of β tends toward 0 when there is no spatial correlation in site energies and thus high disorder and tends toward 1 when the spatial correlation is infinite and disorder is low. The isotropic populations of both MEH-PPV and P3HT in the porous silica hosts have spatial correlation parameters of 0.75 and 0.68, respectively. This is a relatively low long-range spatial correlation, consistent with the idea that these are isolated chromophores, as expected for coiled polymer chains inside defects in the porous hosts. The value is particularly low for P3HT, where π -stacking is frustrated in the isotropic population. The aligned populations of both MEH-PPV and P3HT, on the other hand, have higher spatial correlation parameters of 0.84 and 0.94, respectively. This means that both polymers have less energetic site disorder when the chains are highly aligned parallel to the axis of the pores. This increase in spatial correlation for the aligned population is particularly pronounced for P3HT due to the recovery of more homogeneous π -stacking. As expected, MEH-PPV shows a lower spatial correlation of energetic site disorder in the aligned population, consistent with the idea that regular π -stacking does not occur in this polymer, even for straight chain polymers.

CONCLUSIONS

By comparing populations of P3HT and MEH-PPV, which typically have opposite aggregation behavior, in our system of aligned mesoporous silica, we can better understand the ways in which order without crystallinity changes the exciton spatial coherence in these two prototypical polymers. Encapsulation into mesoporous silica straightens and aligns a significant fraction of the polymer chains in the composite, and by polarizing the excitation light parallel to the pore axis, we can selectively study this aligned but not crystalline population, something that has not been previously possible via traditional film-casting methods. There is also an isotropic population present that can absorb and emit light perpendicular to the pore axis, which we have concluded consists of highly disordered chains comprised mostly of isolated, nonaggregated chromophores.

By isolating the absorption and emission spectra from each of these populations, we can start to understand exactly what physical conformations of the polymer chains result in H- and J-aggregation-like spectral features. For P3HT, we see that the 0–0 shoulder, often observed in the absorption spectrum of highly crystalline spin-coated films, arises not directly from crystallinity but instead from the straightening of the polymer

backbone that leads to increased along-the-chain exciton spatial coherence. In other words, crystallinity can be used to straighten the polymer backbone, but it is straightening of the backbone itself that produces the change in vibronic structure in the spectroscopy of this material, not other features of the crystalline environment. We also see that despite the increased J-like coupling, the aligned population of P3HT in pores is still H-aggregate dominated, so that H-aggregation can occur without crystallization as long as it is promoted by straight, parallel polymer chains. For the predominantly J-aggregated MEH-PPV, however, straightening the polymer backbone does not promote interchain π -stacking or H-like interactions. Instead, the dominant effect of alignment for MEH-PPV is to further increase the J-like coupling by straightening the polymer chains. This increased J-type coupling also increases the exciton coherence size compared to both isotropic polymers in pores and spin-coated films.

Overall, we find that straightening the polymer chains by encapsulation in an aligned mesoporous silica host does not always lead to increased exciton spatial coherence. For J-aggregate polymers like MEH-PPV, we see an increase in exciton spatial coherence for the aligned population because this system is dominated by along-the-chain coupling. Aligning H-aggregate polymers like P3HT, however, actually reduces exciton spatial coherence due to finite-size effects in the pores, leading to shifts in the absorption and PL spectra. The results for both polymers help demonstrate the importance of π -stacking behavior—even without crystallinity—in facilitating 2-D exciton spatial coherence, particularly in H-aggregate dominant polymers.

ASSOCIATED CONTENT

Supporting Information

The Supporting Information is available free of charge at <https://pubs.acs.org/doi/10.1021/acs.jpcc.1c05844>.

Experimental procedures, data analysis procedures, and additional polarized spectroscopic measurements on both host/guest systems and spin-coated polymer films (PDF)

AUTHOR INFORMATION

Corresponding Authors

Sarah H. Tolbert – Department of Chemistry and Biochemistry, University of California, Los Angeles, Los Angeles, California 90095-1569, United States; California NanoSystems Institute, University of California, Los Angeles, Los Angeles, California 90095-7227, United States; Department of Materials Science and Engineering, University of California, Los Angeles, Los Angeles, California 90095-1595, United States; orcid.org/0000-0001-9969-1582; Email: tolbert@chem.ucla.edu

Benjamin J. Schwartz – Department of Chemistry and Biochemistry, University of California, Los Angeles, Los Angeles, California 90095-1569, United States; California NanoSystems Institute, University of California, Los Angeles, Los Angeles, California 90095-7227, United States; orcid.org/0000-0003-3257-9152; Email: schwartz@chem.ucla.edu

Authors

K. J. Winchell – Department of Chemistry and Biochemistry, University of California, Los Angeles, Los Angeles, California 90095-1569, United States

Matthew G. Voss – Department of Chemistry and Biochemistry, University of California, Los Angeles, Los Angeles, California 90095-1569, United States

Complete contact information is available at:

<https://pubs.acs.org/10.1021/acs.jpcc.1c05844>

Author Contributions

K.J.W. and M.G.V. contributed equally to this work.

Notes

The authors declare no competing financial interest.

ACKNOWLEDGMENTS

This work was supported by the National Science Foundation under Grant CHE-2003755. This paper includes work supported by a National Science Foundation Graduate Research Fellowship under Grant DGE-1650604. Any opinion, findings, and conclusions or recommendations expressed in this material are those of the authors and do not necessarily reflect the views of the National Science Foundation. Use of the Stanford Synchrotron Radiation Lightsources, SLAC National Accelerator Laboratory, is supported by the U.S. Department of Energy, Office of Science, Office of Basic Energy Sciences, under Contract DE-AC02-76SF00515. The authors gratefully acknowledge Dr. Hiro Miyata at Canon, Inc., for providing the rub-aligned polyimide substrates.

REFERENCES

- (1) Moliton, A.; Hiorns, R. C. Review of Electronic and Optical Properties of Semiconducting π -Conjugated Polymers: Applications in Optoelectronics. *Polym. Int.* **2004**, *53* (10), 1397–1412.
- (2) Braun, D. Semiconducting Polymer LEDs. *Mater. Today* **2002**, *5* (6), 32–39.
- (3) Wang, Y. J.; Yu, G. Conjugated Polymers: From Synthesis, Transport Properties, to Device Applications. *J. Polym. Sci., Part B: Polym. Phys.* **2019**, *57* (23), 1557–1558.
- (4) Arias, A. C.; MacKenzie, J. D.; McCulloch, I.; Rivnay, J.; Salleo, A. Materials and Applications for Large Area Electronics: Solution-Based Approaches. *Chem. Rev.* **2010**, *110* (1), 3–24.
- (5) Luzio, A.; Criante, L.; D’Innocenzo, V.; Caironi, M. Control of Charge Transport in a Semiconducting Copolymer by Solvent-Induced Long-Range Order. *Sci. Rep.* **2013**, *3*, 1–6.
- (6) Aloui, W.; Adhikari, T.; Nunzi, J. M.; Bouazizi, A.; Khirouni, K. Effect of Thermal Annealing on the Electrical Properties of P3HT:PC70BM Nanocomposites. *Mater. Sci. Semicond. Process.* **2015**, *39*, 575–581.
- (7) Wu, Y.; Schneider, S.; Walter, C.; Chowdhury, A. H.; Bahrami, B.; Wu, H. C.; Qiao, Q.; Toney, M. F.; Bao, Z. Fine-Tuning Semiconducting Polymer Self-Aggregation and Crystallinity Enables Optimal Morphology and High-Performance Printed All-Polymer Solar Cells. *J. Am. Chem. Soc.* **2020**, *142*, 392–406.
- (8) Spano, F. C.; Silva, C. H- and J-Aggregate Behavior in Polymeric Semiconductors. *Annu. Rev. Phys. Chem.* **2014**, *65*, 477–500.
- (9) Österbacka, R.; An, C. P.; Jiang, X. M.; Vardeny, Z. V. Two-Dimensional Electronic Excitations in Self-Assembled Conjugated Polymer Nanocrystals. *Science* **2000**, *287* (5454), 839–842.
- (10) Guo, Z.; Lee, D.; Schaller, R. D.; Zuo, X.; Lee, B.; Luo, T.; Gao, H.; Huang, L. Relationship between Interchain Interaction, Exciton Delocalization, and Charge Separation in Low-Bandgap Copolymer Blends. *J. Am. Chem. Soc.* **2014**, *136* (28), 10024–10032.
- (11) Reid, O. G.; Pensack, R. D.; Song, Y.; Scholes, G. D.; Rumbles, G. Charge Photogeneration in Neat Conjugated Polymers. *Chem. Mater.* **2014**, *26* (1), 561–575.
- (12) Kasha, M. Energy Transfer Mechanisms and the Molecular Exciton Model for Molecular Aggregates. *Radiat. Res.* **1963**, *20* (1), 55.
- (13) Hochstrasser, R. M.; Kasha, M. Application of the Exciton Model To Mono-Molecular Lamellar Systems. *Photochem. Photobiol.* **1964**, *3* (4), 317–331.
- (14) Collison, C. J.; Treemanekarn, V.; Oldham, W. J.; Hsu, J. H.; Rothberg, L. J. Aggregation Effects on the Structure and Optical Properties of a Model PPV Oligomer. *Synth. Met.* **2001**, *119* (1–3), 515–518.
- (15) Clark, J.; Silva, C.; Friend, R. H.; Spano, F. C. Role of Intermolecular Coupling in the Photophysics of Disordered Organic Semiconductors: Aggregate Emission in Regioregular Polythiophene. *Phys. Rev. Lett.* **2007**, *98* (20), 1–4.
- (16) Spano, F. C. Absorption in Regio-Regular Poly(3-Hexyl)-Thiophene Thin Films: Fermi Resonances, Interband Coupling and Disorder. *Chem. Phys.* **2006**, *325* (1), 22–35.
- (17) Collison, C. J.; Rothberg, L. J.; Treemanekarn, V.; Li, Y. Conformational Effects on the Photophysics of Conjugated Polymers: A Two Species Model for MEH-PPV Spectroscopy and Dynamics. *Macromolecules* **2001**, *34* (7), 2346–2352.
- (18) Spano, F. C. The Spectral Signatures of Frenkel Polarons in H- and J-Aggregates. *Acc. Chem. Res.* **2010**, *43* (3), 429–439.
- (19) Hestand, N. J.; Spano, F. C. Expanded Theory of H- and J-Molecular Aggregates: The Effects of Vibronic Coupling and Intermolecular Charge Transfer. *Chem. Rev.* **2018**, *118* (15), 7069–7163.
- (20) Günes, S.; Neugebauer, H.; Sariciftci, N. S. Conjugated Polymer-Based Organic Solar Cells. *Chem. Rev.* **2007**, *107* (4), 1324–1338.
- (21) Hynynen, J.; Kiefer, D.; Müller, C. Influence of Crystallinity on the Thermoelectric Power Factor of P3HT Vapour-Doped with F4TCNQ. *RSC Adv.* **2018**, *8*, 1593–1599.
- (22) Lim, E.; Peterson, K. A.; Su, G. M.; Chabinye, M. L. Thermoelectric Properties of Poly(3-Hexylthiophene) (P3HT) Doped with 2,3,5,6-Tetrafluoro-7,7,8,8-Tetracyanoquinodimethane (F4TCNQ) by Vapor-Phase Infiltration. *Chem. Mater.* **2018**, *30* (3), 998–1010.
- (23) Yamagata, H.; Hestand, N. J.; Spano, F. C.; Köhler, A.; Scharsich, C.; Hoffmann, S. T.; Bässler, H. The Red-Phase of Poly[2-Methoxy-5-(2-Ethylhexyloxy)-1,4-Phenylenevinylene] (MEH-PPV): A Disordered HJ-Aggregate. *J. Chem. Phys.* **2013**, *139* (11), 114903.
- (24) Marcus, M.; Tozer, O. R.; Barford, W. Theory of Optical Transitions in Conjugated Polymers. II. Real Systems. *J. Chem. Phys.* **2014**, *141* (16), 164102.
- (25) Nguyen, T. Q.; Doan, V.; Schwartz, B. J. Conjugated Polymer Aggregates in Solution: Control of Interchain Interactions. *J. Chem. Phys.* **1999**, *110* (8), 4068–4078.
- (26) Nguyen, T. Q.; Martini, I. B.; Liu, J.; Schwartz, B. J. Controlling Interchain Interactions in Conjugated Polymers: The Effects of Chain Morphology on Exciton-Exciton Annihilation and Aggregation in MEH-PPV Films. *J. Phys. Chem. B* **2000**, *104* (2), 237–255.
- (27) Chang, J. F.; Clark, J.; Zhao, N.; Sirringhaus, H.; Breiby, D. W.; Andreasen, J. W.; Nielsen, M. M.; Giles, M.; Heeney, M.; McCulloch, I. Molecular-Weight Dependence of Interchain Polaron Delocalization and Exciton Bandwidth in High-Mobility Conjugated Polymers. *Phys. Rev. B: Condens. Matter Mater. Phys.* **2006**, *74* (11), 115318.
- (28) Scholes, D. T.; Yee, P. Y.; Lindemuth, J. R.; Kang, H.; Onorato, J.; Ghosh, R.; Luscombe, C. K.; Spano, F. C.; Tolbert, S. H.; Schwartz, B. J. The Effects of Crystallinity on Charge Transport and the Structure of Sequentially Processed F4TCNQ-Doped Conjugated Polymer Films. *Adv. Funct. Mater.* **2017**, *27* (44), 1–13.
- (29) Dimitriev, O. P. Effect of Confinement on Photophysical Properties of P3HT Chains in PMMA Matrix. *Nanoscale Res. Lett.* **2017**, *12*, 510.

- (30) Spano, F. C. Modeling Disorder in Polymer Aggregates: The Optical Spectroscopy of Regioregular Poly(3-Hexylthiophene) Thin Films. *J. Chem. Phys.* **2005**, *122* (23), 234701.
- (31) Clark, J.; Chang, J. F.; Spano, F. C.; Friend, R. H.; Silva, C. Determining Exciton Bandwidth and Film Microstructure in Polythiophene Films Using Linear Absorption Spectroscopy. *Appl. Phys. Lett.* **2009**, *94* (16), 163306.
- (32) Yee, P. Y.; Scholes, D. T.; Schwartz, B. J.; Tolbert, S. H. Dopant-Induced Ordering of Amorphous Regions in Regiorandom P3HT. *J. Phys. Chem. Lett.* **2019**, *10* (17), 4929–4934.
- (33) Yin, K.; Zhang, L.; Lai, C.; Zhong, L.; Smith, S.; Fong, H.; Zhu, Z. Photoluminescence Anisotropy of Uni-Axially Aligned Electrospun Conjugated Polymer Nanofibers of MEH-PPV and P3HT. *J. Mater. Chem.* **2011**, *21* (2), 444–448.
- (34) Roehling, J. D.; Arslan, I.; Moulé, A. J. Controlling Microstructure in Poly(3-Hexylthiophene) Nanofibers. *J. Mater. Chem.* **2012**, *22* (6), 2498–2506.
- (35) Camposo, A.; Pensack, R. D.; Moffa, M.; Fasano, V.; Altamura, D.; Giannini, C.; Pisignano, D.; Scholes, G. D. Anisotropic Conjugated Polymer Chain Conformation Tailors the Energy Migration in Nanofibers. *J. Am. Chem. Soc.* **2016**, *138* (47), 15497–15505.
- (36) Niles, E. T.; Roehling, J. D.; Yamagata, H.; Wise, A. J.; Spano, F. C.; Moulé, A. J.; Grey, J. K. J-Aggregate Behavior in Poly-3-Hexylthiophene Nanofibers. *J. Phys. Chem. Lett.* **2012**, *3* (2), 259–263.
- (37) Molenkamp, W. C.; Watanabe, M.; Miyata, H.; Tolbert, S. H. Highly Polarized Luminescence from Optical Quality Films of a Semiconducting Polymer Aligned within Oriented Mesoporous Silica. *J. Am. Chem. Soc.* **2004**, *126*, 4476–4477.
- (38) Miyata, H.; Kuroda, K. Formation of a Continuous Mesoporous Silica Film with Fully Aligned Mesochannels on a Glass Substrate. *Chem. Mater.* **2000**, *12* (1), 49–54.
- (39) Miyata, H.; Kuroda, K. Alignment of Mesoporous Silica on a Glass Substrate by a Rubbing Method. *Chem. Mater.* **1999**, *11* (6), 1609–1614.
- (40) Miyata, H.; Noma, T.; Watanabe, M.; Kuroda, K. Preparation of Mesoporous Silica Films with Fully Aligned Large Mesochannels Using Nonionic Surfactants. *Chem. Mater.* **2002**, *14* (2), 766–772.
- (41) Miyata, H.; Kawashima, Y.; Itoh, M.; Watanabe, M. Preparation of a Mesoporous Silica Film with a Strictly Aligned Porous Structure through a Sol-Gel Process. *Chem. Mater.* **2005**, *17* (21), 5323–5327.
- (42) Fukuoka, A.; Miyata, H.; Kuroda, K. Alignment Control of a Cyanine Dye Using a Mesoporous Silica Film with Uniaxially Aligned Mesochannels. *Chem. Commun.* **2003**, No. 2, 284–285.
- (43) Miyata, H.; Kuroda, K. Film to Fiber Transformation of Preferentially Aligned Mesoporous Silica. *Adv. Mater.* **2001**, *13* (8), 558–561.
- (44) Cadby, A. J.; Tolbert, S. H. Controlling Optical Properties and Interchain Interactions in Semiconducting Polymers by Encapsulation in Periodic Nanoporous Silicas with Different Pore Sizes. *J. Phys. Chem. B* **2005**, *109* (38), 17879–17886.
- (45) Nguyen, T.; Wu, J.; Doan, V.; Schwartz, B. J.; Tolbert, S. H. Control of Energy Transfer in Oriented Conjugated Polymer-Mesoporous Silica Composites. *Science* **2000**, *288* (5466), 652–656.
- (46) Schwartz, B. J.; Nguyen, T. Q.; Wu, J.; Tolbert, S. H. Interchain and Intrachain Exciton Transport in Conjugated Polymers: Ultrafast Studies of Energy Migration in Aligned MEH-PPV/Mesoporous Silica Composites. *Synth. Met.* **2001**, *116* (1–3), 35–40.
- (47) Martini, I. B.; Craig, I. M.; Molenkamp, W. C.; Miyata, H.; Tolbert, S. H.; Schwartz, B. J. Controlling Optical Gain in Semiconducting Polymers with Nanoscale Chain Positioning and Alignment. *Nat. Nanotechnol.* **2007**, *2* (10), 647–652.
- (48) Imanishi, M.; Kajiyama, D.; Koganezawa, T.; Saitow, K. I. Uniaxial Orientation of P3HT Film Prepared by Soft Friction Transfer Method. *Sci. Rep.* **2017**, *7* (1), 1–10.
- (49) Rahimi, K.; Botiz, I.; Agumba, J. O.; Motamen, S.; Stingelin, N.; Reiter, G. Light Absorption of Poly(3-Hexylthiophene) Single Crystals. *RSC Adv.* **2014**, *4* (22), 11121–11123.
- (50) Kohn, P.; Huettner, S.; Komber, H.; Senkovskyy, V.; Tkachov, R.; Kiriya, A.; Friend, R. H.; Steiner, U.; Huck, W. T. S.; Sommer, J. U.; et al. On the Role of Single Regiodefects and Polydispersity in Regioregular Poly(3-Hexylthiophene): Defect Distribution, Synthesis of Defect-Free Chains, and a Simple Model for the Determination of Crystallinity. *J. Am. Chem. Soc.* **2012**, *134* (10), 4790–4805.
- (51) Spano, F. C. Excitons in Conjugated Oligomer Aggregates, Films, and Crystals. *Annu. Rev. Phys. Chem.* **2006**, *57* (1), 217–243.
- (52) Paquin, F.; Yamagata, H.; Hestand, N. J.; Sakowicz, M.; Bérubé, N.; Côté, M.; Reynolds, L. X.; Haque, S. A.; Stingelin, N.; Spano, F. C.; et al. Two-Dimensional Spatial Coherence of Excitons in Semicrystalline Polymeric Semiconductors: Effect of Molecular Weight. *Phys. Rev. B: Condens. Matter Mater. Phys.* **2013**, *88* (15), 155202.
- (53) Spano, F. C.; Yamagata, H. Vibronic Coupling in J-Aggregates and beyond: A Direct Means of Determining the Exciton Coherence Length from the Photoluminescence Spectrum. *J. Phys. Chem. B* **2011**, *115* (18), 5133–5143.
- (54) Spano, F. C.; Clark, J.; Silva, C.; Friend, R. H. Determining Exciton Coherence from the Photoluminescence Spectral Line Shape in Poly(3-Hexylthiophene) Thin Films. *J. Chem. Phys.* **2009**, *130* (7), 074904.
- (55) Engmann, S.; Turkovic, V.; Denner, P.; Hoppe, H.; Gobsch, G. Optical Order of the Polymer Phase within Polymer/Fullerene Blend Films. *J. Polym. Sci., Part B: Polym. Phys.* **2012**, *50* (19), 1363–1373.